J Biomol NMR (2009) 44:107–112
DOI 10.1007/s10858-009-9320-4

NMR STRUCTURE NOTE

Solution structure of the first immunoglobulin domain of human myotilin

Outi Heikkinen · Perttu Permi · Harri Koskela · Olli Carpén · Jari Ylänne · Ilkka Kilpeläinen

Received: 30 January 2009 / Accepted: 1 April 2009 / Published online: 6 May 2009

Abstract Myotilin is a 57 kDa actin-binding and -bundling protein that consists of a unique serine-rich amino-terminus, two Ig-domains and a short carboxy-terminus with a PDZ-binding motif. Myotilin localizes in sarcomeric Z-discs, where it interacts with several sarcomeric proteins. Point mutations in myotilin cause muscle disorders morphologically highlighted by sarcomeric disarray and aggregation. The actin-binding and dimerization propensity of myotilin has been mapped to the Ig-domains. Here we present high-resolution structure of the first Ig-domain of myotilin (MyoIg1) determined with solution state NMR spectroscopy. Nearly complete chemical shift assignments of MyoIg1 were achieved despite several missing backbone ^{1}H-^{15}N-HSQC signals. The structure derived from distance and dihedral angle restraints using torsion angle dynamics was further refined using molecular dynamics. The structure of MyoIg1 exhibits I-type Ig-fold. The absence of several backbone ^{1}H-^{15}N-HSQC signals can be explained by conformational exchange taking place at the hydrophobic core of the protein.

Keywords Myotilin · Immunoglobulin-like domain · Actin-binding protein · Z-disc · NMR · Structure

Biological context

Myotilin, palladin and myopalladin form a small homologous group of cytoskeletal proteins functioning as scaffolds that regulate actin organization (Otey et al. 2005). All these proteins contain multiple immunoglobulin-like (Ig) domains. Myotilin, the founder member of the group, is a

Electronic supplementary material The online version of this article (doi:10.1007/s10858-009-9320-4) contains supplementary material, which is available to authorized users.

O. Heikkinen (✉) · I. Kilpeläinen
Laboratory of Organic Chemistry, Department of Chemistry, University of Helsinki, P.O. Box 55, 00014 Helsinki, Finland
e-mail: Outi.K.Heikkinen@helsinki.fi

P. Permi
Program in Structural Biology and Biophysics, Institute of Biotechnology, University of Helsinki, P.O. Box 65, 00014 Helsinki, Finland

H. Koskela
Finnish Institute for Verification of the Chemical Weapons Convention (VERIFIN), University of Helsinki, A.I. Virtasen aukio 1, P.O. Box 55, 00014 Helsinki, Finland

O. Carpén
Department of Anatomy and Neuroscience Program, Biomedicum, University of Helsinki, P.O. Box 63, 00014 Helsinki, Finland

O. Carpén
Department of Pathology, Helsinki University Hospital, University of Helsinki, 00014 Helsinki, Finland

O. Carpén
Department of Pathology, University of Turku and Turku University Central Hospital, 20520 Turku, Finland

J. Ylänne
Department of Biological and Environmental Science and Nanoscience Center, University of Jyväskylä, P.O. Box 35, 40014 Jyväskylä, Finland

57 kDa actin-binding protein found at sarcomeric Z-discs of both skeletal and cardiac muscle (Salmikangas et al. 1999). It plays a role as structural organizer of the cytoskeleton and it participates in assembly and structural maintenance of the sarcomeric Z-discs. Point mutations in myotilin cause muscle disorders such as limb-girdle muscular dystrophy type 1A and myofibrillar myopathy. Palladin is widely expressed in vertebrate tissues (Parast and Otey 2000; Mykkänen et al. 2001) and plays a role in cell motility e.g. in invasion of metastatic cancer cells (Goicoechea et al. 2008) and in wound healing (Rönty et al. 2006). Myopalladin, the youngest member of the group, is expressed mostly in skeletal muscle (Bang et al. 2001). Myotilin has been shown to bind and cross-link filamentous actin (Salmikangas et al. 2003; von Nandelstadh et al. 2005) and the actin-binding characteristics of palladin were recently characterized in detail (Dixon et al. 2008). Even if myotilin mutations in humans have been noted to cause muscle diseases, the myotilin gene knock-out in mice does not perturb the muscle structure and function (Moza et al. 2007). This result could be an indication of partly complementary roles of myotilin, palladin and myopalladin.

The myotilin sequence is 498 residues in length and it contains two consecutive Ig-domains close to its C-terminus followed by short C-terminal tail (Salmikangas et al. 1999). The unique N-terminal part of myotilin has areas rich of serine residues and it carries potential phosphorylation sites. Myotilin has been shown to interact with actin, α-actinin, filamin C (van der Ven et al. 2000) and FATZ-1/FATZ-2 (Gontier et al. 2005) and recently also with Enigma family proteins (von Nandelstadh et al. 2009). Myotilin cross-links and bundles filamentous actin even though it does not contain a conventional actin-binding domain (von Nandelstadh et al. 2005). The actin-binding propensity of myotilin has been mapped to the Ig-domains. The shortest fragment of myotilin able to bind actin is the second Ig-domain accompanied by short C-terminal tail, but longer constructs are needed for actin bundling. Actin-binding and -bundling seems to be a co-operative act of both Ig-domains. The Ig-domains are also responsible for formation of myotilin homodimers and for the interaction with filamin C. The α-actinin binding site resides at the N-terminal section of myotilin. The disease-causing mutations of myotilin are located to the N-terminal part of the protein and they do not seem to affect the myotilin-actin interaction.

Palladin and myopalladin contain five Ig-domains (Bang et al. 2001; Dixon et al. 2008). The Ig-domains are the most conserved areas between palladin and myopalladin. The Ig-domains 1 and 2 of myotilin are highly homologous to the palladin and myopalladin Ig-domains 4 and 5, respectively. The principal actin-binding domain of palladin seems to be the Ig-domain 3, but Ig-domains 3–4 are required for fully efficient actin binding and bundling. As the actin binding of both myotilin and palladin has been mapped to their Ig-domains, and also some other proteins e.g. kettin have been indicated to use Ig-domains to bind actin, it has been postulated that certain Ig-domains can act as actin-binding modules (von Nandelstadh et al. 2005; Dixon et al. 2008).

We have solved the structure of the first Ig-like domain of myotilin (MyoIg1) using solution state NMR spectroscopy. MyoIg1 participates in myotilin dimerization, in filamin C binding and in myotilin-actin interaction which makes it an important module of myotilin. As the Ig-domains of myotilin and palladin have been shown to act as actin-binding motifs, the structural data on these domains is essential.

Methods and results

Protein production

Human myoIg1 (nucleotide number 1025–1312 corresponding to amino acid residues 249–344, Genbank accession number AF144477, (Salmikangas et al. 1999)) was PCR amplified (forward primer ATATATCCAT GGG ACCACCA CGTTTCATTC AAGTGCCAGA GAAC and reverse primer ATATATATGC GGCCGCTTAT TCTTTT GCAA GGACATCCAG CTGCACAGTG AAGGTG) and cloned to a modified pET24d (Novagen) vector using *Nco*I and *Not*I restriction sites. The insert was verified by DNA sequencing. The plasmid contained a His_6 sequence, followed by glutathione *S*-transferase and tobacco etch virus (TEV) protease cleavage site. After cleavage the final product contained vector-derived residues GAMG before the myotilin sequence. The protein expression was induced with 0.4 mM IPTG in *E. coli* BL21 DE3 for 4 h at 37°C in M9 media containing [$^{13}C_6$]-D-glucose and $^{15}NH_4Cl$ as the sole source of carbon and nitrogen, respectively. Cells were centrifuged, washed twice with and suspended into 20 mM sodium phosphate, 500 mM NaCl, pH 7.4. Cells were broken with French press and cell debris was removed using ultracentrifugation. MyoIg1-GST fusion protein was bound to Glutathione Sepharose 4 fast flow (GE healthcare) and washed with 10 mM sodium phosphate, 140 mM NaCl, pH 7.4. Protein was eluted from the column with 10 mM glutathione, 150 mM NaCl and 50 mM Tris-HCl, pH 8.0. GST tag was cleaved with TEV-protease overnight at 30°C and removed using Ni-NTA agarose (Qiagen). Protein fractions were concentrated with Amicon Centriprep 3000 molecular weight cutoff filter. Gel filtration on Superdex 75 16/60 (GE Healtcare) was performed as final purification step of $^{13}C^{15}N$-MyoIg1 in 20 mM sodium phosphate, 140 mM NaCl, 1 mM dithiothreitol (DTT), pH

7.4. Protein fractions were concentrated with Amicon Centriprep 3000 and Microcon YM-3 filters. The NMR sample used in structure determination contained 1 mM protein in 20 mM sodium phosphate, 140 mM NaCl, 2 mM NaN_3, 1 mM DTT, pH 6.8. The solvent system was 5% (v/v) D_2O in H_2O.

NMR spectroscopy

The NMR spectra for structure determination were recorded with Varian INOVA 600 and 800 MHz spectrometers equipped with 5 mm triple-resonance probe-heads with z-gradients. All NMR experiments were performed at 20°C. Data collection and processing was done using VNMR 6.1C software (Varian Inc., Palo Alto, CA). Conventional set of triple-resonance experiments (HNCA, iHNCA, HN(CO)CA, HNCACB, HN(CO)CACB, HNCO) was used in backbone resonance assignment. Side-chain resonance assignment was based on 3D HCCH-COSY, CC(CO)NH and HCC(CO)NH spectra and on 2D (Hβ)Cβ(CγCδ)Hδ and (Hβ)Cβ(CγCδCε)Hε spectra. The distance restraints were extracted from 3D ^{13}C- and ^{15}N-edited NOESY-HSQC spectra. Sparky 3.011 software (Goddard and Kneller 2004) was used in spectrum visualization.

Twelve backbone amide N–H signals are missing from ^{1}H-^{15}N-HSQC spectrum of MyoIg1 (Fig. 1) which complicated the sequential backbone resonance assignment. The missing signals (R268, V273, V281, I299, V300, E302, K303, S307, L308, C323, F334 and T335) are not located to any specific area but are scattered throughout the sequence. In addition, there are many residues with low ^{1}H-^{15}N-HSQC signal intensity. Some cross-peaks from these problematic residues were also missing from ^{1}H-^{13}C-HSQC spectrum. Except for missing signals, the spectra were of good quality and resonance assignments were found for 98% of all ^{1}H, ^{13}C and ^{15}N nuclei. The resonance assignments of MyoIg1 have been deposited to BioMagResBank under accession number 7113.

Structure determination

The distance restraints for structure calculations were extracted from ^{13}C- and ^{15}N-edited 3D NOESY-HSQC spectra recorded at 800 MHz field. Structure calculation was done using the automatic NOE signal assignment (CANDID method) and torsion angle dynamics mode of CYANA 2.1 software (Herrmann et al. 2002). Assignment was found for 88% of the 3861 NOESY signals. After removal of redundant (e.g. geminal protons), duplicate and unsupported NOEs, 2,016 final distance restraints were generated. Most of the discarded restraints had short-range ($|i-j| \leq 1$) assignments. Proportion of the discarded long-range distance restraints was 12%, which is less than the 20% regarded as the upper limit for reliable CYANA run. The number of distance restraints is good given that many signals were missing from the HSQC spectra. In addition to

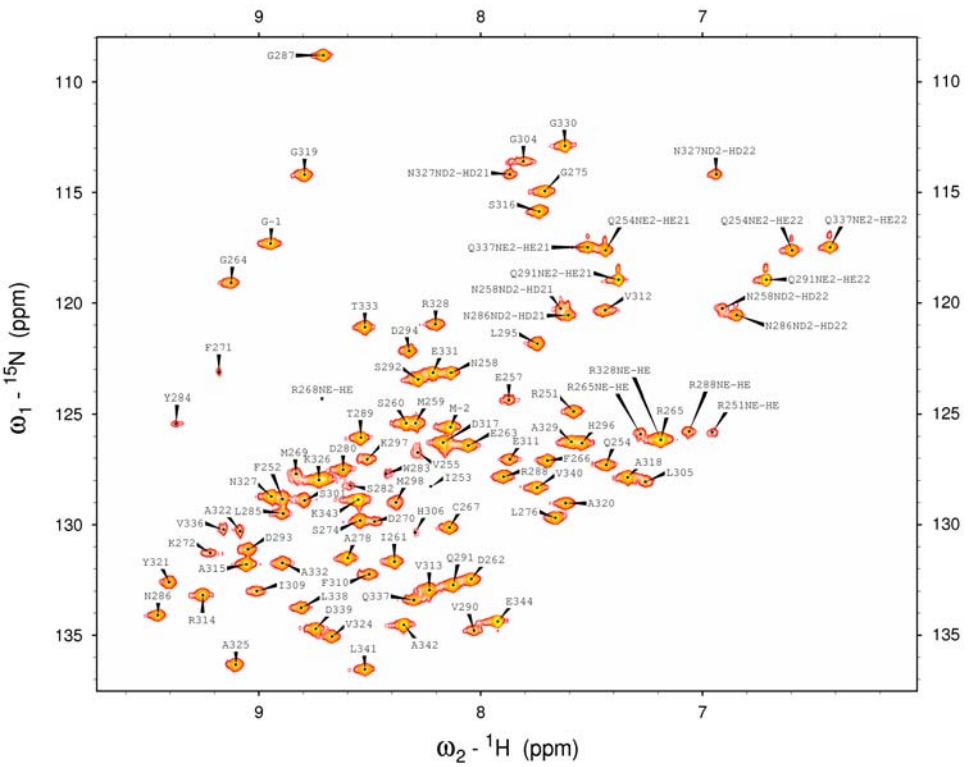

Fig. 1 The 2D ^{1}H-^{15}N-HSQC spectrum of uniformly ^{13}C^{15}N-labeled human MyoIg1 in 20 mM sodium phosphate buffer at pH 6.8 with 140 mM NaCl. The spectrum was recorded at 800 MHz field at 20°C. The resonance assignments of the backbone and side-chain amides are shown. Picture was created with Sparky 3.011 software (Goddard and Kneller 2004)

distance restraints, 138 ψ and ϕ backbone dihedral angle restraints were derived from chemical shift data using TALOS software (Cornilescu et al. 1999). After CYANA calculation there were no violated distance or dihedral angle constraints in the 40 structures chosen from the 400 calculated structures. Selection of the structures was based on lowest target function values. Structures were refined with molecular dynamics using generalized Born implicit solvent model in AMBER 8.0 (Case et al. 2004). After refinement, 25 structures were selected to the final structure ensemble based on lowest AMBER energy and restraint violation energy. The coordinates of the structure family have been deposited to Protein Data Bank under accession code 2KDG.

Table 1 presents the quality parameters of the MyoIg1 structure ensemble. Even if there were a lot of peaks missing from the ^{1}H-^{15}N-HSQC spectrum, nearly complete resonance assignment of the side chain signals was achieved. Thus the structure determination of MyoIg1 was successful and produced a good quality structure. All distance restraint violations fall under 0.2 Å. On average also the dihedral angle violations are small: in 25 substructures only two violations exceed 10°. Rather large violations of 17.1° and 10.1° are encountered with ψ angles of S274 and V336, respectively. However, the average violations for these angles are 1.4° ± 3.8° and 1.0° ± 1.9° (n ± SD), respectively, which indicates that in most of the substructures also these restraints are fulfilled. Both backbone and heavy atom RMSD values of the structure family are very low and coordinate precision is uniform throughout the structure. There are no residues in the disallowed regions of the Ramachandran plot. The structure of MyoIg1 has traditional I-type Ig-fold with 8 β-strands: AA′BCC′DEFG (Fig. 2a). There is also a short 3^{10}-helix between the E and F strands. The surface charge of MyoIg1 shows that the N-terminal end of the Ig-domain is positively charged whereas the C-terminal side is mostly negative (Fig. 2c, d).

Table 1 Structural statistics for MyoIg1 (25 structures)

Total distance restraints	2,016
Short-range $\|i - j\| \leq 1$	1,000
Medium-range, $1 < \|i - j\| < 5$	229
Long-range, $\|i - j\| \geq 5$	787
Restraints per residue	20.2
Violation statistics	
Maximum NOE restraint violation (Å)	0.17
Number of NOE violations >0.1 Å (n ± SD)	1.0 ± 0.0
Maximum dihedral angle constraint violation (°)	17.1
Number of dihedral angle constraint violations >5° (n ± SD)	1.0 ± 0.8
Energies	
Average AMBER energy (kcal/mol ± SD)	−4,068.11 ± 6.33
Average restraint violation energy (kcal/mol ± SD)	7.33 ± 0.87
RMS deviations from ideal covalent geometry	
Bond lengths (Å ± SD)	0.0100 ± 0.0001
Bond angles (° ± SD)	2.06 ± 0.02
Atomic coordinate RMSD (Å) for residues 249–342	
Backbone atoms	0.36 ± 0.05
Heavy atoms	0.76 ± 0.07
Ramachandran map regions (%)	
Residues in most favored regions	86.9
Additionally allowed regions	13.1
Generously allowed regions	0.0
Disallowed regions	0.0

Discussion and conclusions

We have presented here a high resolution solution structure of the first immunoglobulin-like domain of myotilin. Our structure of MyoIg1 exhibits typical I-type Ig-fold. According to structural similarity search on DALI server (Holm and Sander 1993) the five closest structures to MyoIg1 are found in titin (PDB accession code 1YA5 and 2F8V), aortic preferentially expressed protein-1 (PDB accession code 1U2H), telokin (PDB accession code 1TLK), palladin (PDB accession code 2DM2) and myomesin (PDB accession code 2R15) all with pairwise RMSD of 1.5–2.0 Å. These all are clearly I-type Ig-domains. Based on sequence comparison the myotilin Ig-domains have been previously predicted to fold as C2-type Ig-domains (Salmikangas et al. 1999). Dixon et al. (2008) proposed that the palladin Ig-domains, which have also been originally predicted to have C2-type Ig-fold, fold as I-type domains. I-type fold is seen in the structures of palladin Ig-domains 1 and 2 which are available in the PDB database (PDB accession codes 2DM2 and 2DM3). As the Ig-domains of the myotilin/palladin/myopalladin protein family are sequentially closest relatives to each other, it is most probable that all 2–5 Ig-domains in the individual proteins of the family belong to the I-class.

During resonance assignment we noted that many signals are missing or have low intensity in the ^{1}H-^{15}N-HSQC spectrum of MyoIg1 (Fig. 1). Sequentially these were not concentrated to any specific area, but the location in the three-dimensional structure shows a clear trend (Fig. 3). To our surprise the low-intensity residues are not situated at the loop areas but practically all of them are located in the most structured areas in the middle of the β-sheets and many of them even participate in formation of the hydrophobic core. The broadening of the ^{1}H-^{15}N-HSQC signals is obviously not due to chemical exchange of the amide protons with

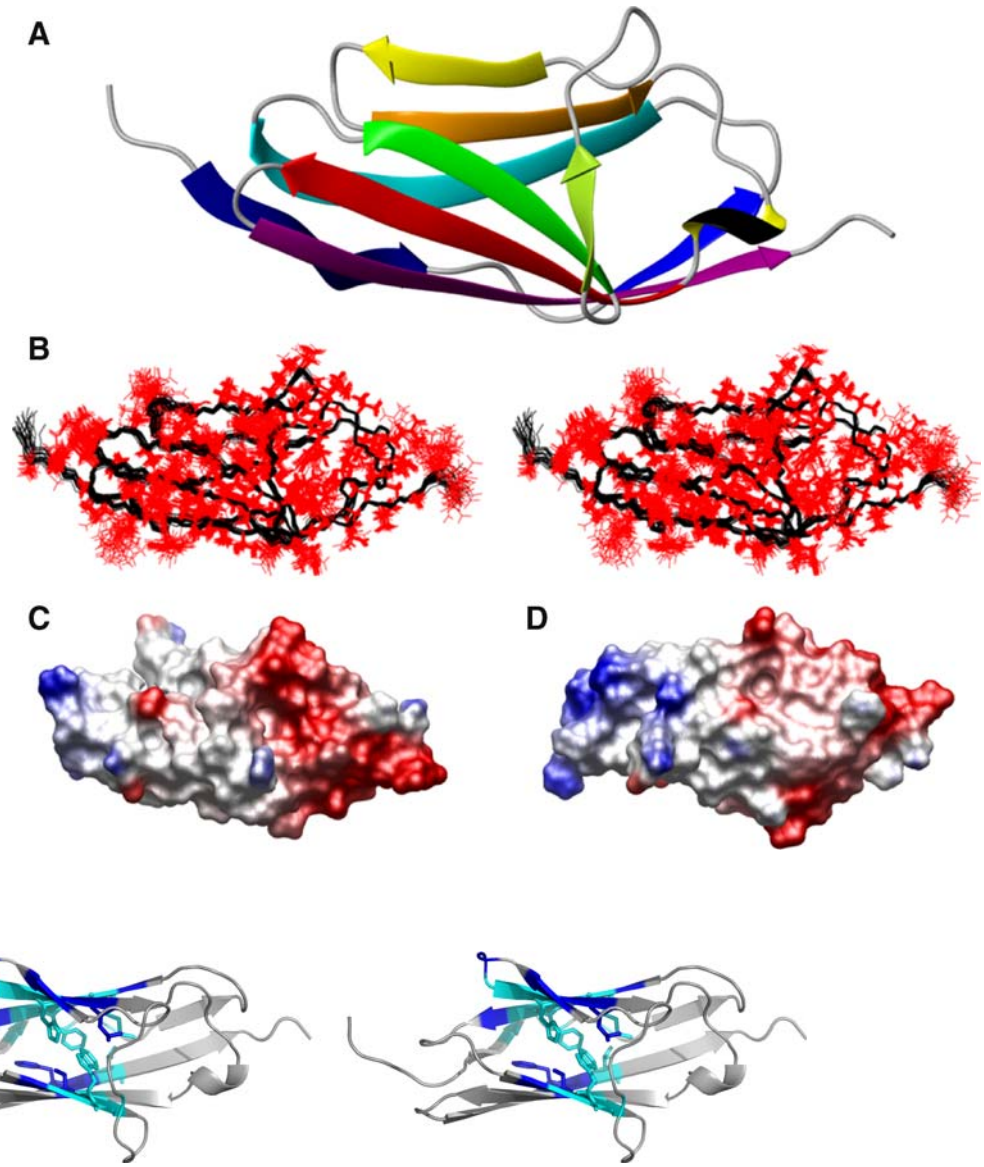

Fig. 2 Solution structure of MyoIg1. **a** Ribbon presentation of the secondary structure. Coloring of the β strands: A—*navy*; A′—*blue*; B—*cyan*; C—*green*; C′—*light green*; D—*yellow*; E—*orange*; F—*red*; G—*purple*. **b** *Stereoview* showing the superimposed backbone traces and the side chains of the structure ensemble (25 structures). Pictures **a** and **b** were created with MOLMOL software (Koradi et al. 1996). **c** and **d** Surface charge. *Blue* = positive, *red* = negative. **c** has same perspective as **a** and **b**. **d** shows the back view: Structure in **c** is rotated 180° along the longitudinal axis. Picture was created with Bodil software (Lehtonen et al. 2004)

Fig. 3 Stereo-view showing the location of the MyoIg1 residues with low intensity ^{1}H-^{15}N-HSQC signals. *Blue*—signal not detected in ^{1}H-^{15}N-HSQC spectrum, *cyan*—low intensity ^{1}H-^{15}N-HSQC signal. Some of the hydrophobic core residues are shown with stick representation. Most of the low-intensity signals are located in the core of the protein. Picture was created with PyMOL software (DeLano Scientific, Palo Alto, CA, USA)

water but it stems from conformational exchange. This conformational exchange is probably taking place at the hydrophobic core of the protein. Modelfree analysis of the backbone amide relaxation data confirmed that these residues undergo millisecond time scale conformational exchange. (see Supplementary Material for ^{15}N R_1 and R_2 relaxation rates, heteronuclear NOEs, backbone amide proton exchange rates and internal motional parameters). The W283 at the C strand is a potential candidate to be the moving residue affecting the integrity of the whole structure (Fig. 3). The side chain of W283 points into the hydrophobic core and contacts many other residues which have low ^{1}H-^{15}N-HSQC signal intensity. In addition to the weak backbone ^{1}H-^{15}N-HSQC signal the indole N–H signal and CT-^{1}H-^{13}C-HSQC peaks of the aromatic side-chain of W283 are also invisible. However, they were detected in ^{13}C-edited NOESY-HSQC spectrum which enabled resonance assignment and extraction of structural restraints.

The Ig-domain 3 has been proven to be the main actin-binding domain of palladin but both domains 3–4 are needed for the fully functional interaction (Dixon et al. 2008). The cooperative action of these two palladin Ig-domains resembles the actin-binding and -bundling function of the myotilin Ig-domains. The Ig-domain 2 seems to be the major actin-binding domain of myotilin and Ig-domain 1 alone does not directly interact with actin

but still the full actin-bundling activity requires both Ig-domains (von Nandelstadh et al. 2005). Structure determination of the actin-binding Ig-domain 3 of palladin is actively going on both with NMR spectroscopy (Dixon and Campbell 2008) and X-ray crystallography (Liang et al. 2006). Further structural data on the actin-binding Ig-domains will give more clues about actin binding interface and bundling mechanism of these novel actin-binding modules.

Acknowledgments Authors would like to thank Minna Leuanniemi and Arja Mansikkaviita for excellent technical assistance on protein production and purification. Outi Heikkinen would like to acknowledge The Finnish National Graduate School in Informational and Structural Biology (ISB) for support. The project has been supported by Academy of Finland systems biology program grant (105211 to J.Y.).

References

Bang M-L, Mudry RE, McElhinny AS, Trombitás K, Geach AJ, Yamasaki R, Sorimachi H, Granzier H, Gregorio CC, Labeit S (2001) Myopalladin, a novel 145-kilodalton sarcomeric protein with multiple roles in Z-disc and I-band protein assemblies. J Cell Biol 153:413–427

Case DA, Darden TA, Cheatham TEIII, Simmerling CL, Wang J, Duke RE, Luo R, Merz KM, Wang B, Pearlman DA, Crowley M, Brozell S, Tsui V, Gohlke H, Mongan J, Hornak V, Cui G, Beroza P, Schafmeister C, Caldwell JW, Ross WS, Kollman PA (2004) AMBER 8. University of California, San Francisco

Cornilescu G, Delaglio F, Bax A (1999) Protein backbone angle restraints from searching a database for chemical shift and sequence homology. J Biomol NMR 13:289–302

Dixon RDS, Campbell SL (2008) ^{1}H, ^{15}N, and ^{13}C NMR chemical shift assignments for the Ig3 domain of palladin. Biomol NMR Assign 2:51–53

Dixon RDS, Arneman DK, Rachlin AS, Sundaresan NR, Costello MJ, Campbell SL, Otey CA (2008) Palladin is an actin cross-linking protein that uses immunoglobulin-like domains to bind filamentous actin. J Biol Chem 283:6222–6231

Goddard TD, Kneller DG (2004) Sparky 3. University of California, San Francisco

Goicoechea SM, Arneman D, Otey CA (2008) The role of palladin in actin organization and cell motility. Eur J Cell Biol 87:517–525

Gontier Y, Taivainen A, Fontao L, Sonnenberg A, van der Flier A, Carpén O, Faulkner G, Borradori L (2005) The Z-disc proteins myotilin and FATZ-1 interact with each other and are connected to the sarcolemma via muscle-specific filamins. J Cell Sci 118: 3739–3749

Herrmann T, Güntert P, Wüthrich K (2002) Protein NMR structure determination with automated NOE assignment using the new software CANDID and the torsion angle dynamics algorithm DYANA. J Mol Biol 319:209–227

Holm L, Sander C (1993) Protein structure comparison by alignment of distance matrices. J Mol Biol 233:123–138

Koradi R, Billeter M, Wüthrich K (1996) MOLMOL: a program for display and analysis of macromolecular structures. J Mol Graph 14:51–55

Lehtonen JV, Still DJ, Rantanen VV, Ekholm J, Björklund D, Iftikhar Z, Huhtala M, Repo S, Jussila A, Jaakkola J, Pentikäinen O, Nyrönen T, Salminen T, Gyllenberg M, Johnson M (2004) BODIL: a molecular modeling environment for structure-function analysis and drug design. J Comput Aided Mol Des 18: 401–419

Liang W, Yang H, Xue X, Huang Q, Bartlamb M, Chena S (2006) Expression, crystallization and preliminary X-ray studies of the immunoglobulin-like domain 3 of human palladin. Acta Cryst F62:556–558

Moza M, Mologni L, Trokovic R, Faulkner G, Partanen J, Carpén O (2007) Targeted deletion of the muscular dystrophy gene myotilin does not perturb muscle structure or function in mice. Mol Cell Biol 27:244–252

Mykkänen O-M, Grönholm M, Rönty M, Lalowski M, Salmikangas P, Suila H, Carpén O (2001) Characterization of human palladin, a microfilament-associated protein. Mol Biol Cell 12:3060–3073

Otey CA, Rachlin A, Moza M, Arneman D, Carpén O (2005) The palladin/myotilin/myopalladin family of actin-associated scaffolds. Int Rev Cytol 246:31–58

Parast MM, Otey CA (2000) Characterization of palladin, a novel protein localized to stress fibers and cell adhesions. J Cell Biol 150:643–655

Rönty M, Leivonen S-K, Hinz B, Rachlin A, Kähäri V-M, Otey C, Carpén O (2006) Isoform specific regulation of palladin, an actin-organizing protein, during TGF-β1-induced myofibroblast differentiation. J Invest Dermatol 126:2387–2396

Salmikangas P, Mykkänen O-M, Grönholm M, Heiska L, Kere J, Carpén O (1999) Myotilin, a novel sarcomeric protein with two Ig-like domains, is encoded by a candidate gene for limb-girdle muscular dystrophy. Hum Mol Gen 8:1329–1336

Salmikangas P, van der Ven P, Lalowski M, Taivainen A, Zhao F, Suila H, Schröder R, Lappalainen P, Fürst D, Carpén O (2003) Myotilin, the limb-girdle muscular dystrophy 1A (LGMD1A) protein, cross-links actin filaments and controls sarcomere assembly. Hum Mol Gen 12:189–203

van der Ven PFM, Wiesner S, Salmikangas P, Auerbach D, Himmel M, Kempa S, Hayeß K, Pacholsky D, Taivainen A, Schröder R, Carpén O, Fürst DO (2000) Indications for a novel muscular dystrophy pathway: γ-filamin, the muscle-specific filamin isoform, interacts with myotilin. J Cell Biol 151:235–247

von Nandelstadh P, Grönholm M, Moza M, Lamberg A, Savilahti H, Carpén O (2005) Actin-organising properties of the muscular dystrophy protein myotilin. Exp Cell Res 310:131–139

von Nandelstadh P, Ismail M, Gardin C, Suila H, Zara I, Belgrano A, Valle G, Carpen O, Faulkner G (2009) A class III PDZ binding motif in myotilin and FATZ families binds Enigma family proteins—a common link for Z-disc myopathies. Mol Cell Biol 29:822–834